Electronic Supplementary Material (ESI) for Dalton Transactions.
This journal is © The Royal Society of Chemistry 2019

Supporting Information

Modulating Absorption and Charge Transfer in Bodipy-Carbazole Donor-Acceptor Dyads through Molecular Design

John Strahan[a], *Bhooshan C. Popere*[b,d], *Piyachai Khomein*[b], *Craig Pointer*[c], *Shea Martin*[c], *Amanda N. Oldacre*[c], *S. Thayumanavan*[b]*, *Elizabeth R. Young*[c]*

a. Department of Chemistry, Amherst College, Amherst, Massachusetts 01002, USA. Fax: +1-413-542-2735

b. Department of Chemistry, University of Massachusetts, Amherst, Massachusetts 01003, USA. E-mail:thai@chem.umass.edu; Fax: +1-413-545-4490

c. Department of Chemistry, Lehigh University, Bethlehem, Pennsylvania 18015, USA. Email: ery317@lehigh.edu; Fax: +1-610-758-6536

d. Current address: The Dow Chemical Company, 455 Forest Street, Marlborough, MA 01752

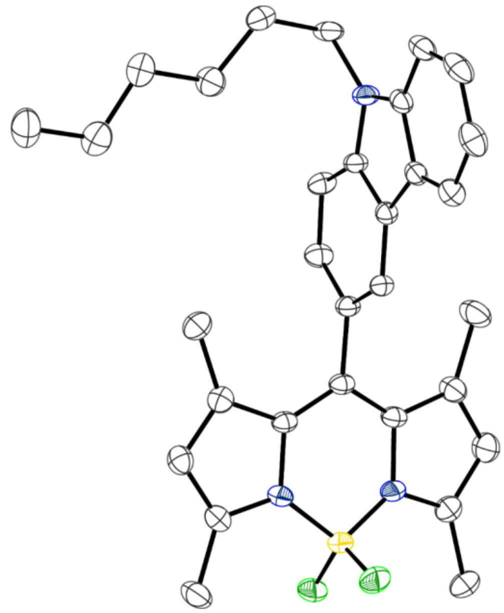

Figure S1. Oak Ridge Thermal Ellipsoid Plot (ORTEP) of ***meso*****BDP-Carb** at the 30% probability level. Hydrogen atoms removed for clarity.

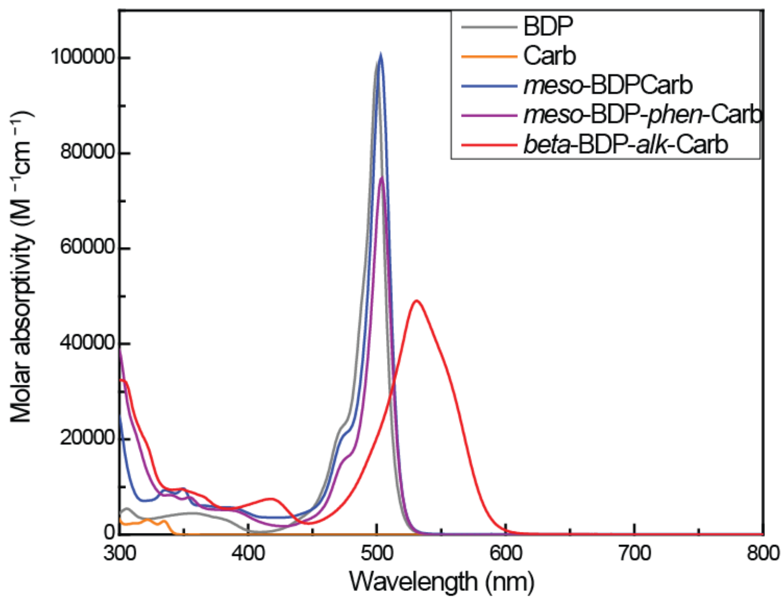

Figure S2. UV-visible absorption spectra in molar absorptivity extending to the UV region for each BDP-Carb dyad as well as the unsubsituted BDP and carbazole moieties.

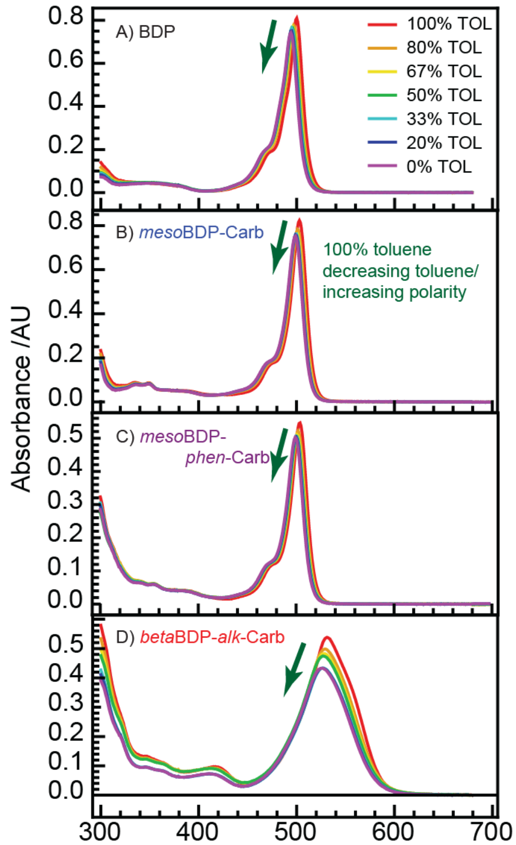

Figure S3. Solvent polarity dependence of absorption spectra of A) **BDP**, B) **mesoBDP-Carb**, C) **mesoBDP-*phen*-Carb**, D) **betaBDP-*alk*-Carb**. Samples were 2 μM in the solvent ratio of toluene/acetonitrile indicated in the legend (shifting from red as the most non-polar to blue as the most polar in rainbow order, and as indicated by the green arrow).

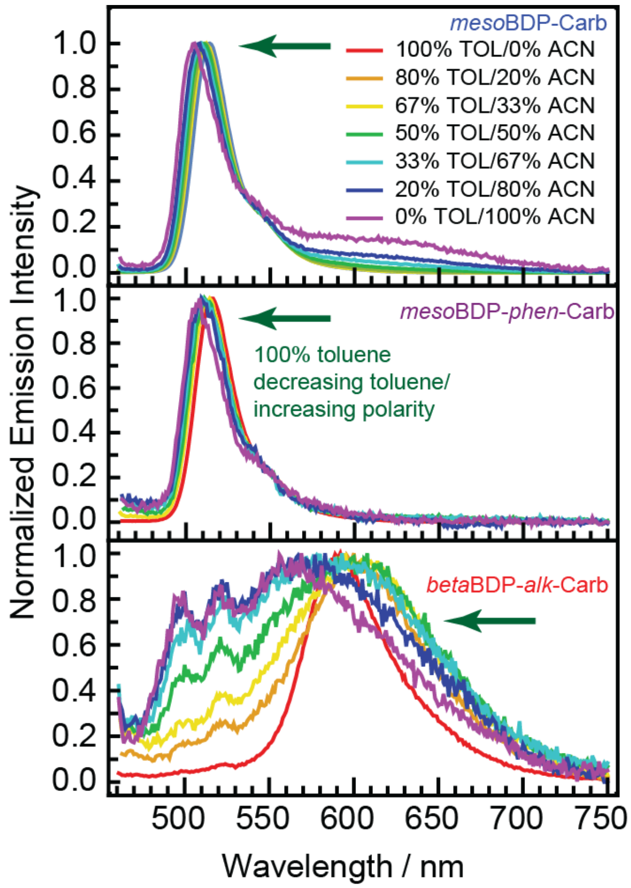

Figure S4. Normalized emission spectra showing solvent polarity dependence. Samples were 0.1 μM in the solvent ratio of toluene/acetonitrile indicated in the legend (shifting from red as the most non-polar to blue as the most polar in rainbow order). Samples were excited at 450 nm.

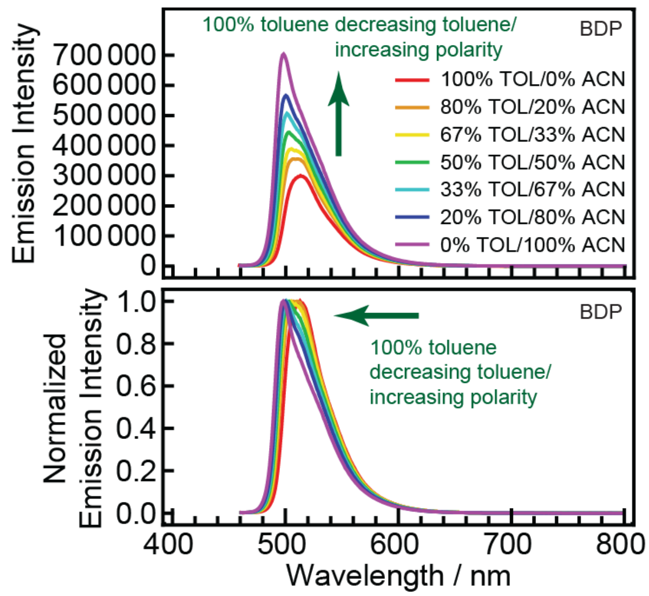

Figure S5. Solvent polarity dependence of emission spectra of BDP (top) and normalized emission intensity (bottom). Samples were 0.1 μM in the solvent ratio of toluene/acetonitrile indicated in the legend (shifting from red as the most non-polar to blue as the most polar in rainbow order). Samples were excited at 450 nm.

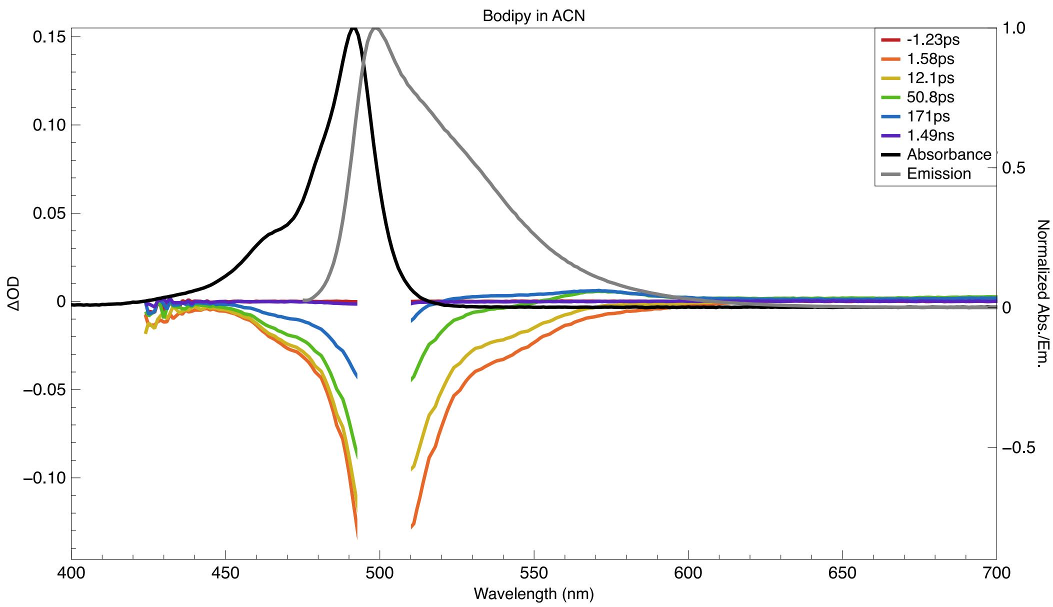

Figure S6. Overlay of transient absorption spectra with the steady-state absorption (black) and emission (grey) spectra for BDP in acetonitrile. Gaps in the spectra correspond to removal of scatter laser excitation light around 500 nm.

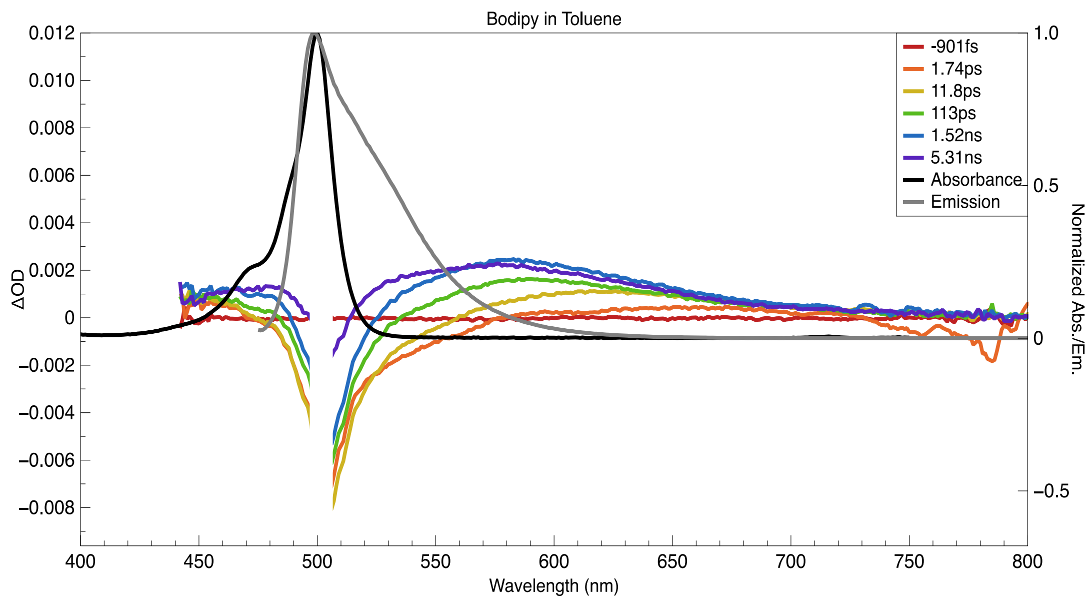

Figure S7. Overlay of transient absorption spectra with the steady-state absorption (black) and emission (grey) spectra for BDP in toluene. Gaps in the spectra correspond to removal of scatter laser excitation light around 500 nm.

Wavelength / nm

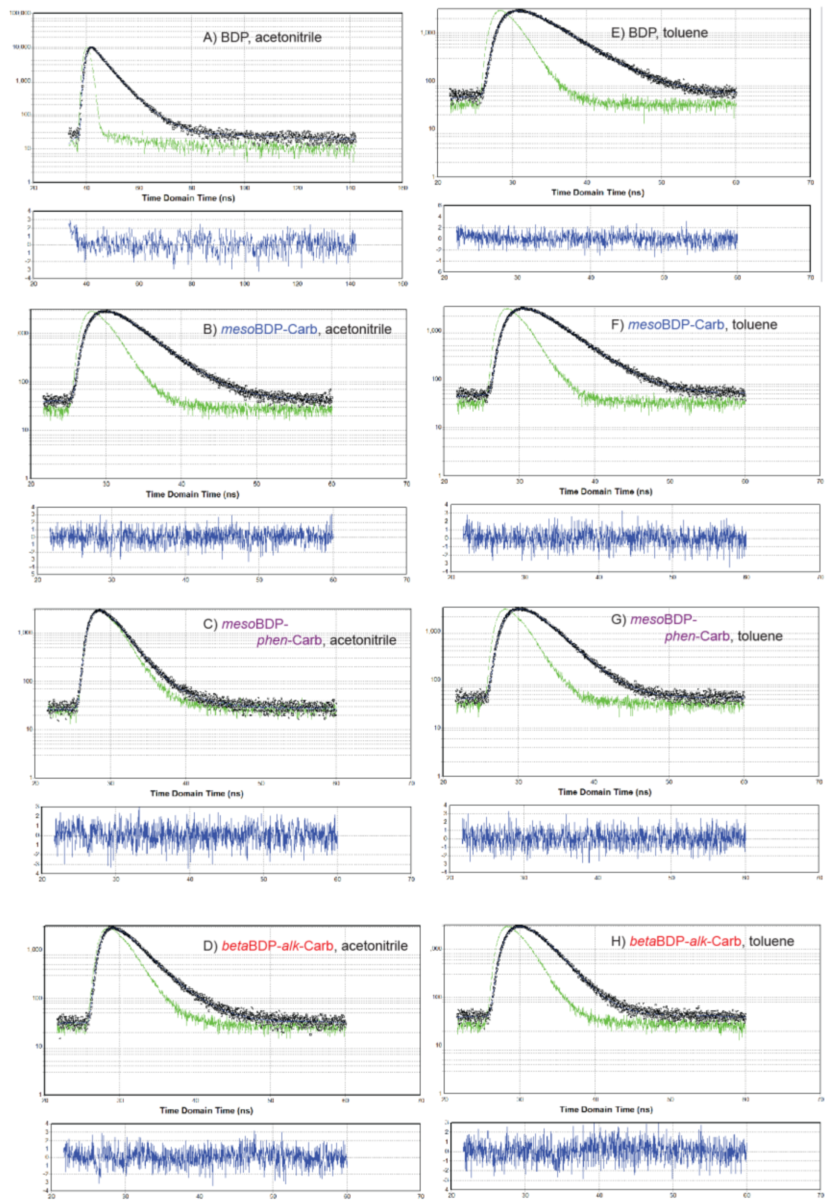

Figure S8. Time-correlated single photon counting (TCSPC) data. TCSPC data (black dots) are deconvolved from the instrument response function, IRF (green line). Fits are shown for each set of data (blue line, matching well with the black dots of data). Residuals (blue lines in lower tile) are shown in the tile below each set of data. The extracted lifetimes are summarized Table 2 for both solvents. Samples (~ 0.1 μM) were prepared in an inert glovebox environment a 1-cm quartz cuvette. The cuvettes were sealed to preserve an air-free sample and removed from the glovebox for experiments. Measurements were collected in acetonitrile (left tiles) and toluene (right tiles). Samples were excited with a 470 nm pulsed nanoLED and the entire emission spectrum was integrated to produce the emission decay trace. A 500-nm long pass filter was used to remove scattered excitation. Lifetimes were extracted by fitting a convolution of the IRF (green trace) and a multiexponential decay to the data using ISS Vinci2 software.

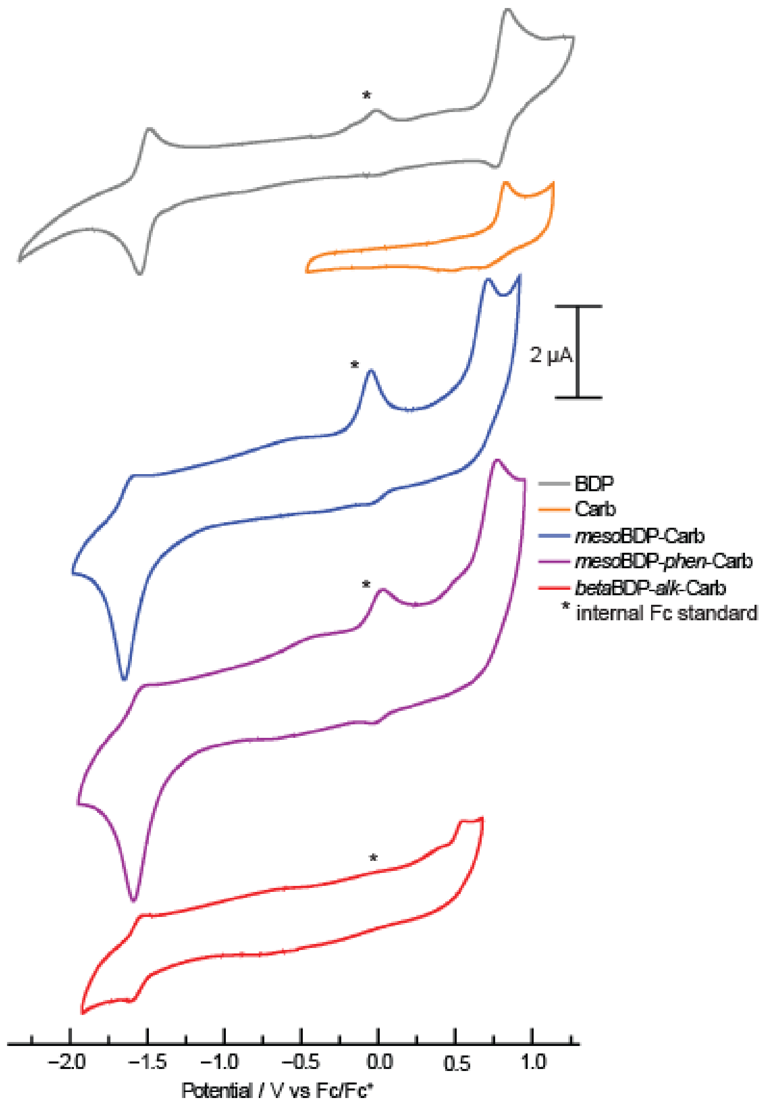

Figure S9. Cyclic voltammograms of 60 μM BDP, Carb, and each BDP-Carb dyad in 0.1 M $TBABF_4$ in acetonitrile. Voltammetry scans were recorded with a platinum working electrode, a platinum counter electrode, and a silver wire quasi reference electrode using an internal ferrocene standard.

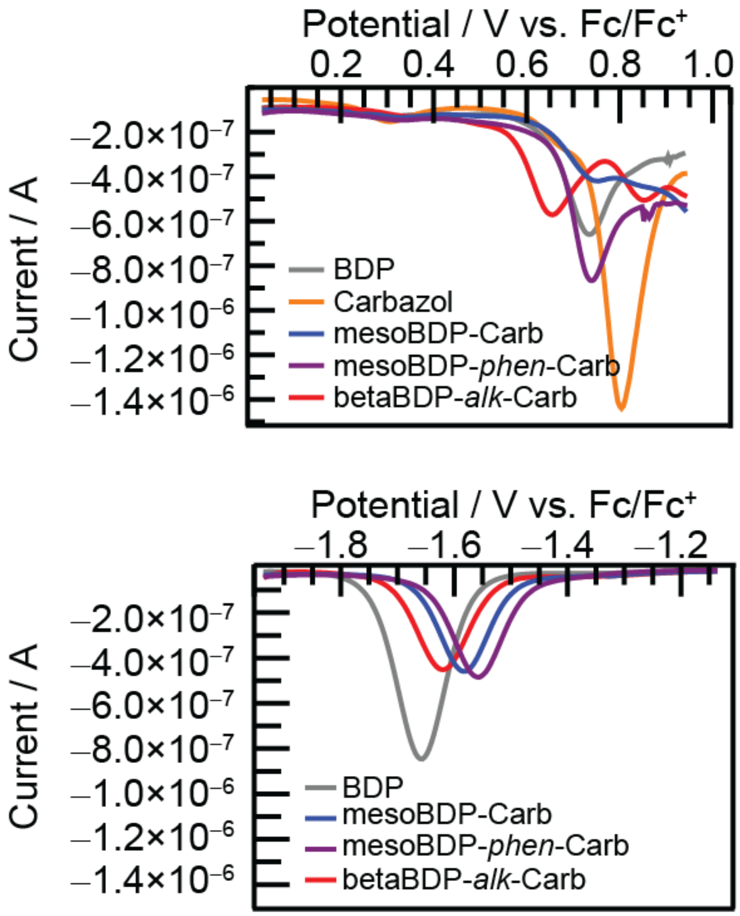

Figure S10. Differential pulse voltammagrams of 60 μM BDP, Carb, and each BDP-Carb dyad in 0.1 M $TBABF_4$ in acetonitrile. Voltammetry scans were recorded with a platinum working electrode, a platinum counter electrode, and a silver wire quasi reference electrode using an internal ferrocene standard. Top tile represents oxidative scans, bottom tile represents reductive scans.

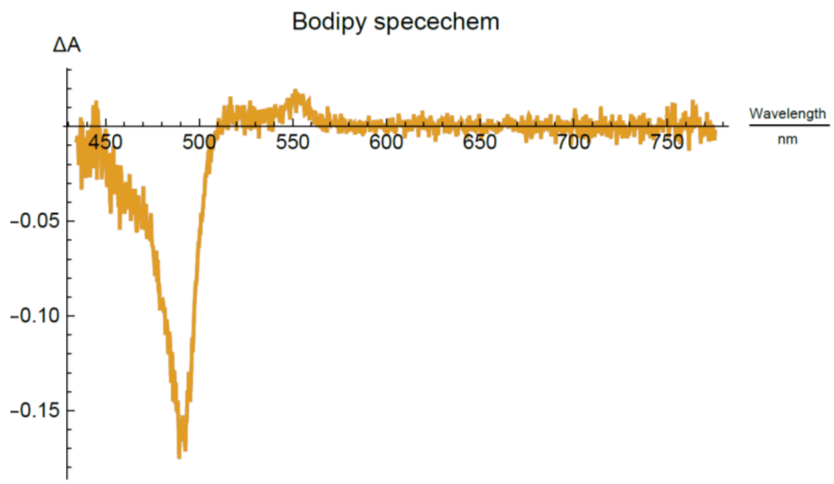

Figure S11. Reductive spectroelectrochemistry of BDP alone. Spectroelectrochemistry was performed using a 30 μM solution of BDP in 0.1 M $TBABF_4$ in acetonitrile using a platinum mesh working electrode, a platinum counter electrode, and a silver wire quasi-reference electrode. Samples were prepared and experiments were performed in an inert glovebox environment.

Calculated Molecular Orbital from Density Functional Theory

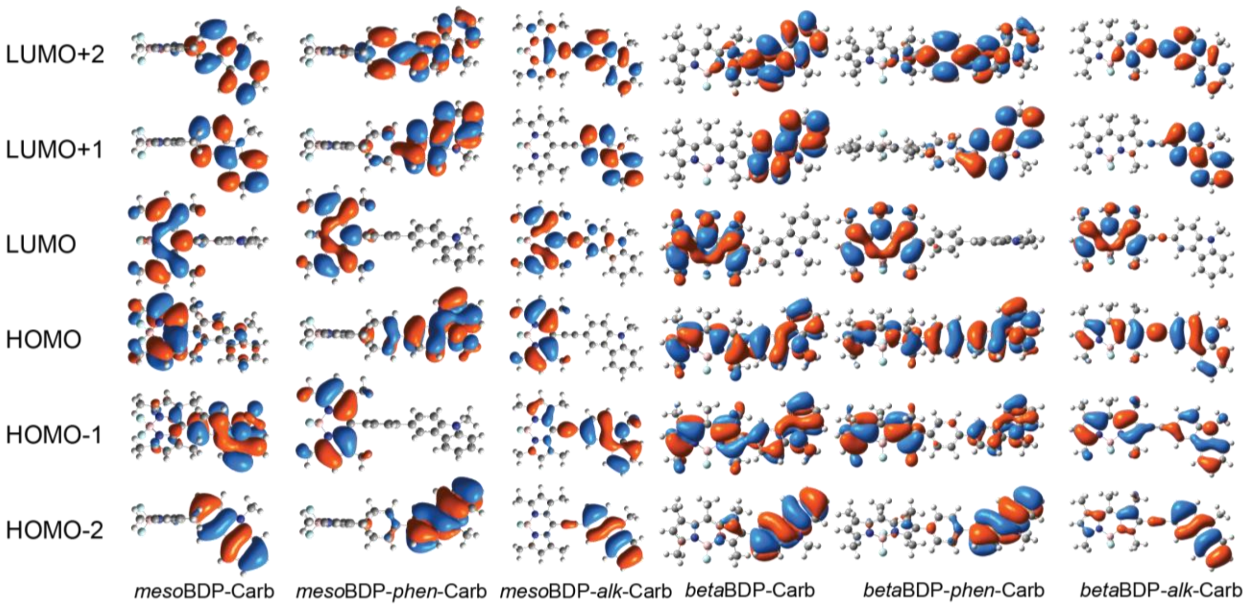

Calculated Orbital Energies from Density Functional Theory

Molecule	HOMO-1	HOMO	LUMO	LUMO+1	Δ LUMO-HOMO
BDP	–4.32	–3.55	–0.25	3.31	3.30
*beta*BDP-Carb	-5.87	-5.56	-2.67	-1.25	2.89
*beta*BDP-*alk*-Carb	–5.98	–5.39	–2.78	–1.31	2.61
*beta*BDP-*phen*-Carb	-5.80	-5.55	-2.70	-1.26	2.85
*meso*BDP-Carb	–5.83	-5.77	–2.74	-1.34	3.03
*meso*BDP-*alk*-Carb	-5.82	-5.81	-3.03	-1.42	2.78
*meso*BDP-*phen*-Carb	–5.95	-5.67	–2.91	-1.21	2.76

DFT orbital energies, reported versus vacuum in units of eV.

Figure S12. Molecular orbitals energy levels obtained from DFT calculations using the ORCA quantum chemistry package the B3LYP functional and a def2-TZVP basis set. Calculations were performed in vacuum. HOMO and LUMO energy levels yield insight to the trends observed in experimental UV-visible spectroscopy.

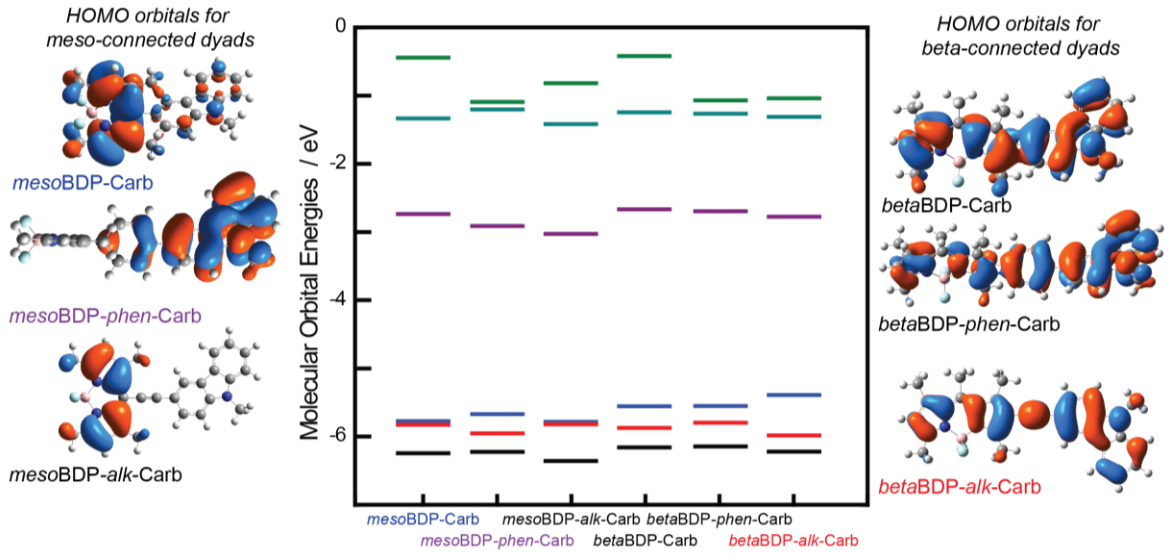

Figure S13. Plotted molecular orbitals energy levels and corresponding HOMO orbitals obtained from DFT calculations with Gaussian using the B3LYP functional and a def2-TZVP basis set.

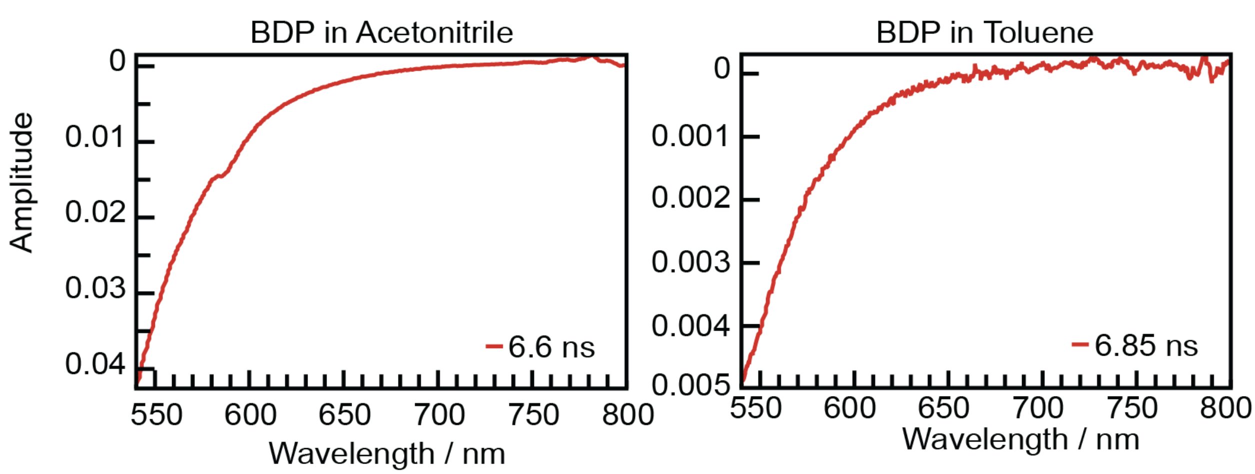

Figure S14. Global analysis DADS of BDP in acetonitrile and toluene.

Experimental Details

Instrumentation

^{1}H and ^{13}C NMR spectra were recorded on a 500 (125) MHz Bruker NMR spectrometer using the residual resonance of the solvent as the internal standard. Chemical shifts are reported in parts per million (ppm). When peak multiplicities are given, the following abbreviations are used: s, singlet; d, doublet; t, triplet; m, multiplet; b, broad. Molar absorptivity was acquired with Cary 5000 UV-vis-NIR spectrometer. ATR-FT-IR data was obtained with a Thermo Scientific Nicolet iS10 with an ATR attachment.

Materials and Synthetic Procedures

All reagents were obtained from commercial sources used as received without further purification, unless otherwise specified. Air- and moisture-sensitive reactions were conducted in oven-dried glassware using a standard Schlenk line or dry box techniques under an inert atmosphere of dry nitrogen. THF was dried over sodium and collected *via* distillation immediately prior to use. *N*,*N*-diisopropylamine was dried over anhydrous calcium hydride, collected by distillation under reduced pressure and stored in airtight Strauss' flasks under a positive argon pressure.

5.6.3 Detailed Synthetic Procedures

***meso*-methyl BODIPY (1)**[1]

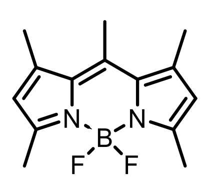

To a solution of 2,4-dimethylpyrrole (2 g, 21 mmol) in dry CH_2Cl_2 (20 mL) was added acetyl chloride (3.84 g, 49 mmol) dropwise at room temperature over 30 min. The resulting deep-red solution was heated to reflux for 1 h. After cooling, the reaction mixture was poured into 50 mL hexanes and the resulting orange suspension was concentrated to dryness. The resulting dypirrin hydrochloride was used without further purification. This was then dissolved in dry CH_2Cl_2 (100 mL) and to this solution was added Et_3N (8.9 mL, 63 mmol) and the solution was stirred at room temperature for 10 min. Subsequently, $BF_3.OEt_2$ (11.5 mL, 91 mmol) was added to the flask slowly, but not dropwise, and the reaction mixture was stirred at room temperature for 1 h. The deep red solution was washed with saturated aq. Na_2CO_3 solution, dried over anhydrous $MgSO_4$ and concentrated *in vacuo*. The crude product was then purified by silica gel chromatography using Combiflash Rf-200 automated flash chromatograph with hexanes-CH_2Cl_2 as the eluents. The product was further purified *via* recrystallization from CH_2Cl_2/MeOH to yield long orange crystals (1.9 g, 70%). UV-vis (toluene): λ_{max} = 500 nm, ε = 98,000 $M^{-1}cm^{-1}$ ATR-FT-IR (cm^{-1}): 2985 (w, sp^3 C–H) ^{1}H NMR (500 MHz $CDCl_3$): δ ppm 6.05 (*s*, 2H), 2.57 (*s*, 3H), 2.52 (*s*, 6H), 2.41 (*s*, 6H).

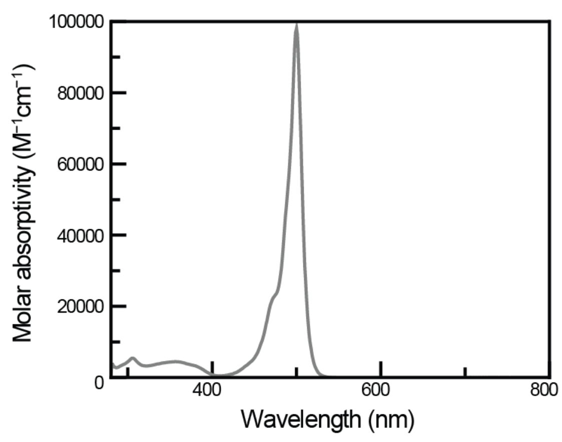

Figure S14. UV-Vis (molar absorptivity) of ***meso*-methyl BODIPY** in toluene

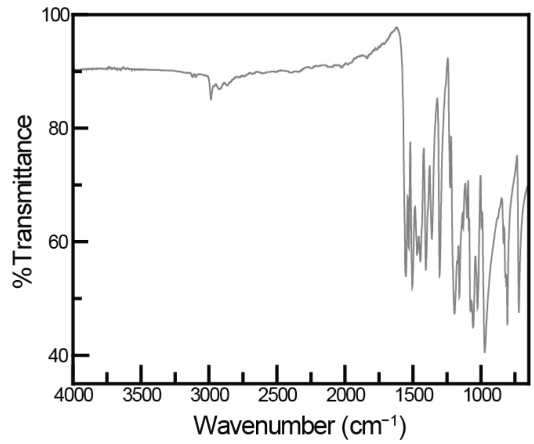

Figure S15. ATR-FT-IR of ***meso*-methyl BODIPY**

2-Iodo *meso*-methyl BDP (2)[2]

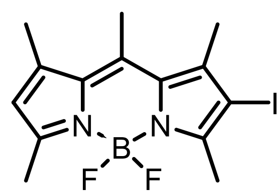

BDP **1** (350 mg, 1.33 mmol) was dissolved in dry CH_2Cl_2 (200 mL). *N*-iodosuccinimide (330 mg, 1.5 mmol) was dissolved in DMF (5 mL) and added dropwise to the stirring solution of **1** at room temperature. The reaction was stirred for 12 h after which, it was quenched with water. The crude product was extracted into ether. The organic fractions were dried over anhydrous $MgSO_4$ and concentrated *in vacuo*. The crude product was then purified by silica gel chromatography using Combiflash Rf-200 automated flash chromatograph with hexanes-CH_2Cl_2 as the eluents. The product was further purified *via* recrystallization from CH_2Cl_2/MeOH to yield an orange solid (355 mg, 70%). ^{1}H NMR (400 MHz, $CDCl_3$): δ ppm 6.12 (*s*, 1H), 2.61 (*s*, 3H), 2.60 (*s*, 3H), 2.53 (*s*, 3H), 2.45 (*s*, 3H), 2.43 (*s*, 3H).

3-Bromocarbazole[3]

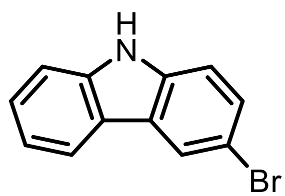

To a suspension of carbazole (2 g, 12 mmol) in DMF (10 mL) was added a solution of *N*-bromosuccinimide (2.1 g, 11.9 mmol) in DMF (10 mL) was added dropwise at 0°C. The reaction mixture was warmed to room temperature and stirred for additional 5 h. The reaction was quenched with water and the product was extracted with CH_2Cl_2. The organic fractions were dried over $MgSO_4$ and dried over anhydrous $MgSO_4$. The crude product was then purified by silica gel chromatography using Combiflash Rf-200 automated flash chromatograph with hexanes-ethyl acetate as the eluents. Solvents were removed *in vacuo* and the resulting white solid was used as such without further analysis for the next reaction.

3-Bromo-*N*-hexylcarbazole (4)[3]

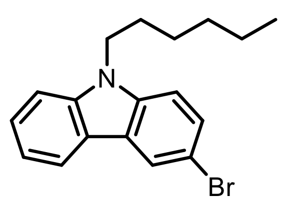

A solution of 3-bromo carbazole (2.3 g, 9.5 mmol) in DMF (100 mL) and anhydrous K_2CO_3 (2.6 g, 19 mmol) was added 1-bromohexane (1.89 g, 11.5 mmol). The reaction was stirred at 80°C for 12 h. After cooling the reaction was quenched with water and the crude product was extracted with ethyl acetate. The organic fraction was dried over anhydrous $MgSO_4$ and concentrated *in vacuo*. The crude product was then purified by silica gel chromatography using Combiflash Rf-200 automated flash chromatograph with hexanes as the eluents. The solvent was evaporated under reduced pressure to yield a waxy white solid (1.5 g, 50%). ^{1}H NMR (400 MHz; $CDCl_3$): δ ppm 8.20 (*d*, *J* = 2.0 Hz, 1H), 8.05 (*d*, *J* = 7.8 Hz, 1H), 7.53 (*dd*, *J* = 8.6, 2.0 Hz, 1H), 7.51 (*m*, *J* = 1.2 Hz, 1H), 7.40 (*d*, *J* = 8.2 Hz, 1H), 7.29-7.27 (*m*, 1H), 7.26-7.22 (*m*, 1H), 4.27 (*t*, *J* = 7.3 Hz, 2H), 1.88 (*m*, 2H), 1.39-1.26 (*m*, 6H), 0.87 (*t*, *J* = 7.1 Hz, 3H).

***N*-Hexyl-2-(4,4,5,5-tetramethyl-1,3,2-dioxaborolan-2-yl)-carbazole (5)**

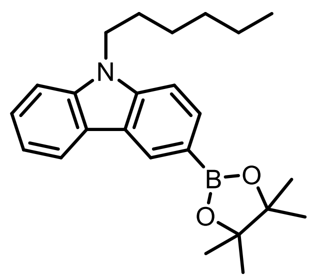

A solution of 3-bromo-*N*-hexyl carbazole (**4)** (1 g, 3 mmol) in dry THF (30 mL) was cooled to –78°C. To this *n*BuLi (2.4 mL, 1.6 M in hexanes, 3.9 mmol) was added dropwise and the reaction was stirred for 1 h after which, it was warmed to room temperature. The reaction mixture was once again cooled to –78°C and 2-isopropoxy-4,4,5,5-tetramethyl-1,3,2-dioxaborolane (0.84 g, 4.5 mmol) was added. The reaction mixture was allowed to warm to room temperature and was stirred for 12 h, after which it was quenched with water. The crude product was extracted with ethyl acetate. The organic fraction was dried over anhydrous $MgSO_4$ and concentrated *in vacuo*. The crude product was then purified by silica gel chromatography using Combiflash Rf-200 automated flash chromatograph with hexanes-ethyl acetate as the eluents. Evaporation of the solvents afforded a pale yellow oil (0.74 g, 65%). ^{1}H NMR (400 MHz; $CDCl_3$): δ ppm 8.63 (*t*, *J* = 0.9 Hz, 1H), 8.16 (*d*, *J* = 7.7 Hz, 1H), 7.95 (*dd*, *J* = 8.2, 1.2 Hz, 1H), 7.51-7.47 (*m*, *J* = 1.2 Hz, 1H), 7.44-

7.41 (*m*, 2H), 7.29-7.25 (*m*, 1H), 4.33 (*t*, *J* = 7.3 Hz, 2H), 1.89 (*quintet*, *J* = 7.4 Hz, 2H), 1.43 (*s*, 12H) 1.35-1.29 (*m*, 6H), 0.88 (*t*, *J* = 7.1 Hz, 3H).

_N_-Hexylcarbazole-3-carbaldehyde (6)[4]

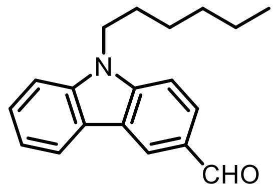

A solution of 3-bromo-*N*-hexyl carbazole (**4**) (3 g, 9 mmol) in anhydrous THF (200 mL) was cooled to –78°C. nBuLi (6.8 mL, 1.6 M in hexanes, 10.9 mmol) was added dropwise and the reaction was allowed to warm to room temperature. After stirring for 30 min at room temperature, DMF (1.7 mL, 22 mmol) was added to the reaction mixture and was stirred for an additional 2 h. The mixture was then quenched with 2M HCl (15 mL) and the crude product was extracted with diethyl ether. The organic fractions were dried over anhydrous MgSO4 and concentrated in vacuo. The crude product was then purified by silica gel chromatography using Combiflash Rf-200 automated flash chromatograph with hexanes-ethyl acetate as the eluents. Evaporation of the solvents under reduced pressure afforded a pale yellow oil (1.9 g, 75%). ^{1}H NMR (300 MHz, $CDCl_3$): δ ppm 10.10 (*s*, 1H), 8.62 (*d*, *J* = 1.5 Hz, 1H), 8.16 (*d*, *J* = 7.8 Hz, 1H), 8.01 (*dd*, *J* = 8.6Hz, 1H), 7.57–7.44 (*m*, 3H), 7.33 (*m*, 1H), 4.34 (*t*, J = 7.2 Hz, 2H), 1.90 (*m*, 2H), 1.38–1.25 (*m*, 6H), 0.87 (*t*, *J* = 7.1 Hz, 3H).

2-trimethylsilylethynyl BDP

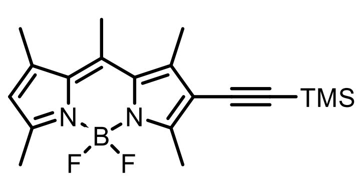

2-Iodo BDP **2** (250 mg, 0.64 mmol) was dissolved in *N*,*N*-diisopropyl amine (10 mL). To this solution were added $Pd(PPh_3)_2Cl_2$ (23 mg, 5 mol%) and CuI (12 mg, 10%) and the contents were purged with Ar. Trimethylsilylacetylene (0.18 mL, 1.28 mmol) was syringed into the flask and the reaction was heated to 90°C for 6 h. The solvent was evaporated and the crude product was purified by silica gel chromatography using Combiflash Rf-200 automated flash chromatograph with hexanes-CH_2Cl_2 as the eluents. Evaporation of the solvents yielded an orange-red solid (200 mg, 56%). ^{1}H NMR (400 MHz; $CDCl_3$): δ ppm 6.10 (*s*, 1H), 2.59 (*s*, 6H), 2.53 (*s*, 3H), 2.48 (*s*, 3H), 2.42 (*s*, 3H), 0.26 (*s*, 9H).

2-ethynyl BODIPY (3)

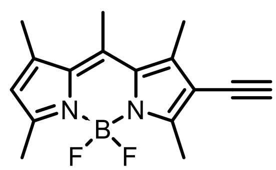

2-trimethylsilylethynyl BDP (200 mg, 0.6 mmol) was dissolved in freshly distilled THF (10 mL), purged with argon and the solution was cooled to –70 °C. A solution of TBAF in THF (1M) (1.9 mL, 1.9 mmol) was added dropwise *via* a syringe over 10 minutes. The reaction mixture was then removed from the cooling bath and stirred at room temperature for 3h. The reaction was then quenched with dilute acetic acid (pH 4) and the crude product was extracted with dichloromethane. The organic layer was dried over anhydrous sodium sulfate and concentrated under reduced pressure. The crude product was then purified by silica gel chromatography using Combiflash Rf-200 automated flash chromatograph with hexanes-dichloromethane as the eluents. The solvents were evaporated *in vacuo* to give the final product as a deep red solid (120 mg, yield 70%). ^{1}H NMR (400 MHz; $CDCl_3$): δ ppm 6.10 (*s*, 1H), 3.34 (*s*, 1H), 2.60 (*s*, 3H), 2.57 (*s*, 3H), 2.53 (*s*, 3H), 2.47 (*s*, 3H), 2.41 (*s*, 3H).

***beta*BDP-*alk*-Carb (9)**

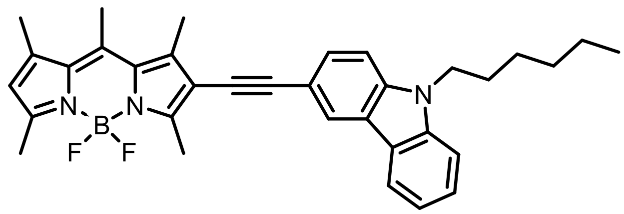

2-ethynyl BODIPY **3** (100 mg, 0.35 mmol) and 3-bromo-*N*-hexylcarbazole **4** (230 mg, 0.7 mmol) were dissolved in anhydrous THF (5 mL) and *N*,*N*-diisopropyl amine (5 mL). To this solution were added $Pd(PPh_3)_2Cl_2$ (12 mg, 5 mol%) and CuI (7 mg, 10%), and the contents were purged with Ar. The reaction was allowed to proceed at 90°C for 6 h. The solvent was evaporated and the crude product was purified by silica gel chromatography using Combiflash Rf-200 automated flash chromatograph with hexanes-ethyl acetate as the eluents. Evaporation of the solvents yielded an orange-red solid (60 mg, 38%). UV-vis (toluene): λ_{max} = 531 nm, ε = 50,000 $M^{-1}cm^{-1}$ ATR-FT-IR (cm^{-1}): 3057-3045 (w, sp^2 C–H), 2984-2807 (s, sp^3 C–H), 2207 (w, C≡C) ^{1}H NMR (500 MHz; $CDCl_3$): δ ppm 8.27 (*dd*, *J* = 1.6, 0.5 Hz, 1H), 8.11 (*d*, *J* = 7.8 Hz, 1H), 7.62 (*dd*, *J* = 8.4, 1.6 Hz, 1H), 7.49-7.47 (*m*, 1H), 7.42 (*d*, *J* = 8.3 Hz, 1H), 7.37 (*dd*, *J* = 8.5, 0.5 Hz, 1H), 7.28-7.24 (*m*, 1H), 6.10 (*s*, 1H), 4.30 (*t*, *J* = 7.3 Hz, 2H), 2.73 (*s*, 3H), 2.64 (*s*, 3H), 2.61 (*s*, 3H), 2.55 (*s*, 3H), 2.44 (*s*, 3H), 1.91-1.84 (*m*, 2H), 1.35-1.31 (*m*, 4H), 0.87 (*t*, *J* = 7.0 Hz, 3H). ^{13}C {^{1}H} NMR (125 MHz $CDCl_3$): δ ppm 155.20, 142.17, 141.66, 140.79, 132.92, 131.15, 129.73, 129.10. 126.10, 123.70, 122.85, 122.45, 121.95, 120.58, 119.30, 115.72, 113.50, 112.08, 110.43, 108.96, 108.77. 97.16, 79.97, 43.23, 31.62, 29.77, 22.61, 17.58, 16.72, 16.11, 14.64, 16.10, 14.64, 14.10, 13.64

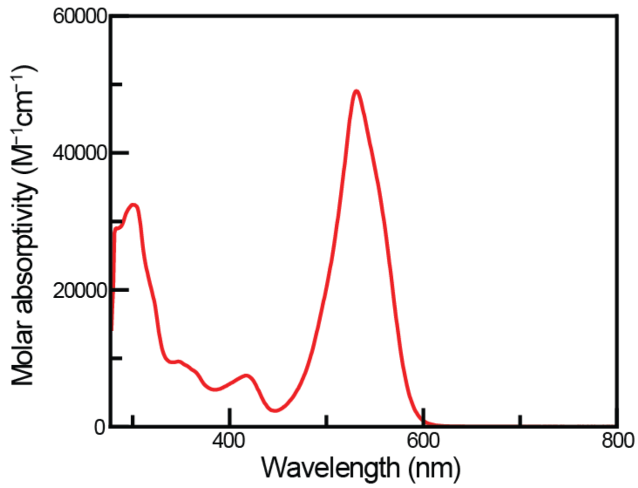

Figure S16. UV-Vis (molar absorptivity) of ***beta*BDP-*alk*-Carb** in toluene

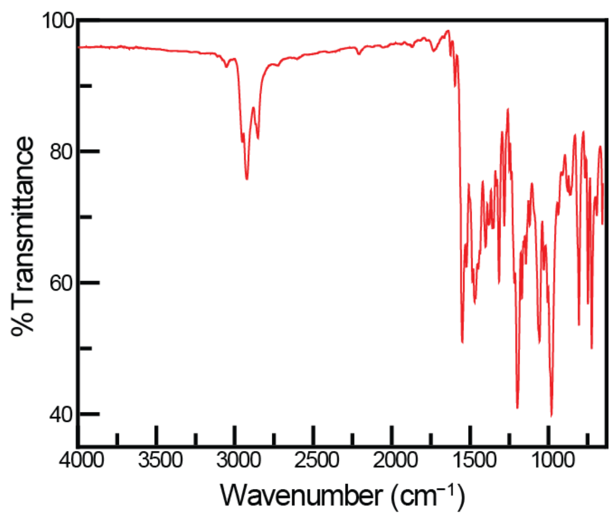

Figure S17. ATR-FT-IR of ***beta*BDP-*alk*-Carb**

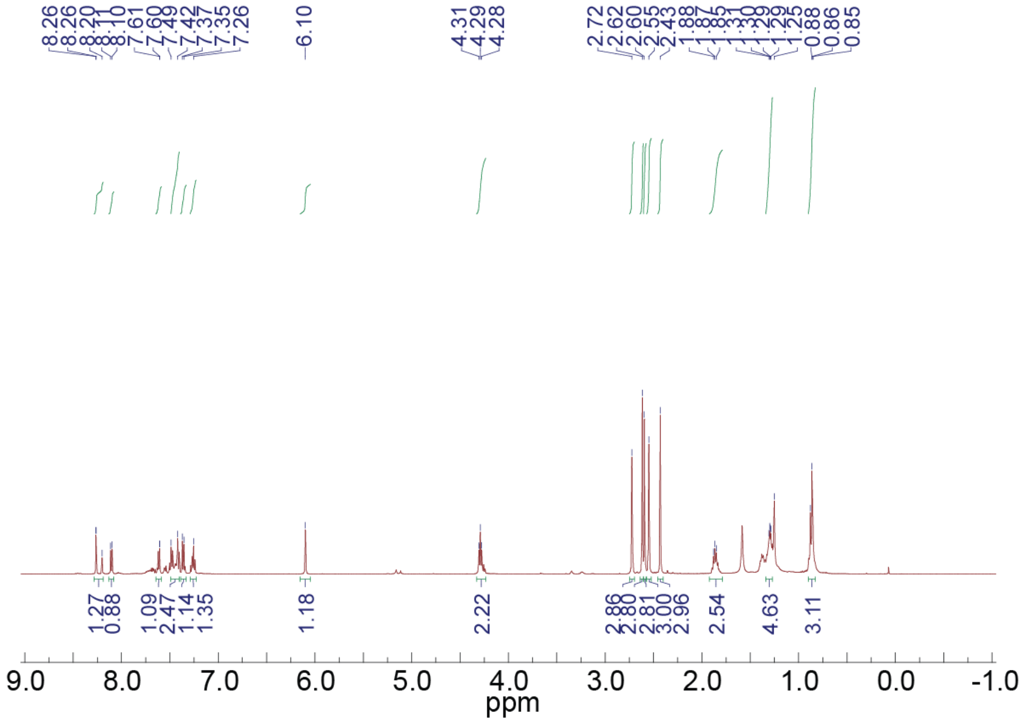

Figure S18. ^{1}H NMR of ***beta*****BDP-*****alk*****-Carb**

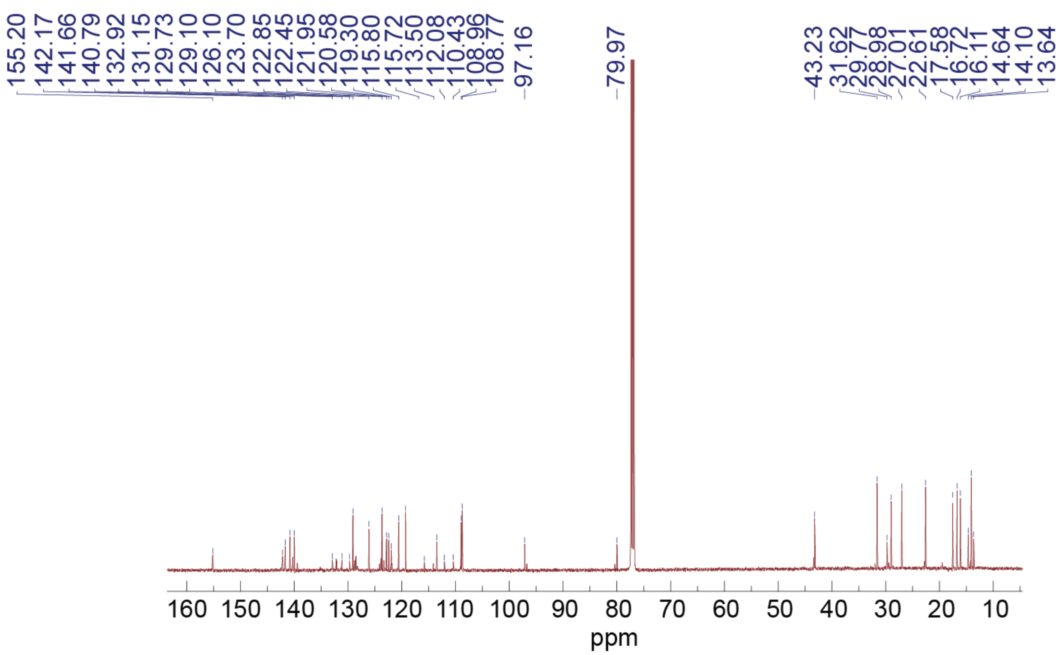

Figure S19. ^{13}C of ***beta*****BDP-*****alk*****-Carb**

***meso*BDP-Carb (7)**

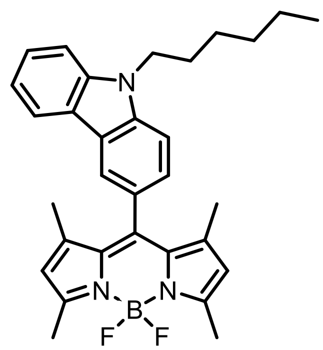

N-Hexylcarbazole-3-carbaldehyde **6** (0.7 g, 2.6 mmol) was dissolved in dry CH_2Cl_2 (200 ml) and the solution was sparged with Ar. 2,4-dimethylpyrrole (0.5 g, 5.25 mmol) was added *via* a syringe and the contents were sparged for additional 5 min. Trifluoroacetic acid (0.1 mL) was added to the flask and the contents were stirred at room temperature for 1.5 h. The reaction was then quenched with 0.1 N NaOH solution and the organic fraction was washed with water, dried over anhydrous $MgSO_4$ and concentrated *in vacuo*. The residue was dissolved in dry toluene (12 mL) and the flask was purged with Ar. Chloranil (723 mg, 2.9 mmol) was added all at once and the reaction was stirred at room temperature for 5 min. Then, Et_3N (3 mL) and $BF_3.OEt_2$ (3 mL) were added at once and the reaction was stirred for 1.5 h. The reaction mixture was concentrated under reduced pressure and the residue was purified by silica gel chromatography using Combiflash Rf-200 automated flash chromatograph with hexanes-ethyl acetate as the eluents. Evaporation of the solvents yielded the product as an orange-red solid (200 mg, 16%). UV-vis (toluene): λ_{max} = 503 nm, ε = 100,000 $M^{-1}cm^{-1}$ ATR-FT-IR (cm^{-1}): 3060-3038 (w, sp^2 C–H) 2990-2812 (s, sp^3 C–H) ^1H NMR (500 MHz; $CDCl_3$): *δ* ppm 8.07 (*d*, *J* = 7.7 Hz, 1H), 7.99 (*d*, *J* = 1.2 Hz, 1H), 7.54-7.51 (*m*, 2H), 7.48 (*d*, *J* = 8.1 Hz, 1H), 7.33 (*dd*, *J* = 8.3, 1.6 Hz, 1H), 7.29-7.25 (*m*, 1H), 5.98 (*s*, 2H), 4.36 (*t*, *J* = 7.2 Hz, 2H), 2.59 (*s*, 6H), 1.93 (*quintet*, *J* = 7.3 Hz, 2H), 1.45-1.38 (*m*, 6H), 1.32 (*s*, 6H), 0.87 (*t*, *J* = 7.1 Hz, 3H). $^{13}C\ \{^{1}H\}$ NMR (125 MHz $CDCl_3$): δ ppm 155.15, 143.49, 143.31, 140.81, 140.66, 132.38, 126. 36, 125.33, 125.13, 123.31, 122.64, 121.14, 120.64, 120.04, 119.36, 109.49, 109.20, 43.43, 31.65, 29.06, 27.16, 22.71, 14.76, 14.12

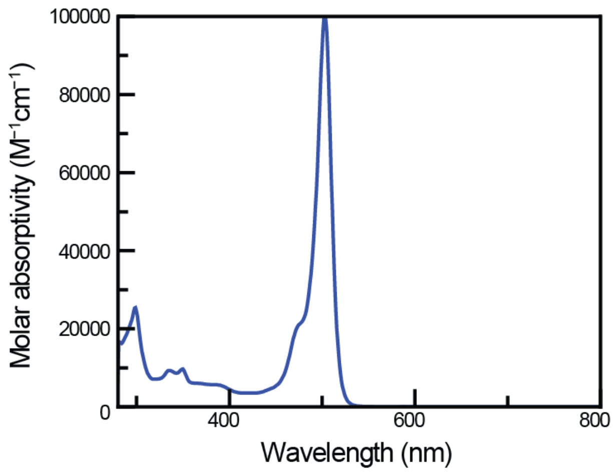

Figure S20. UV-Vis (molar absorptivity) of ***meso*BDP-Carb** in toluene

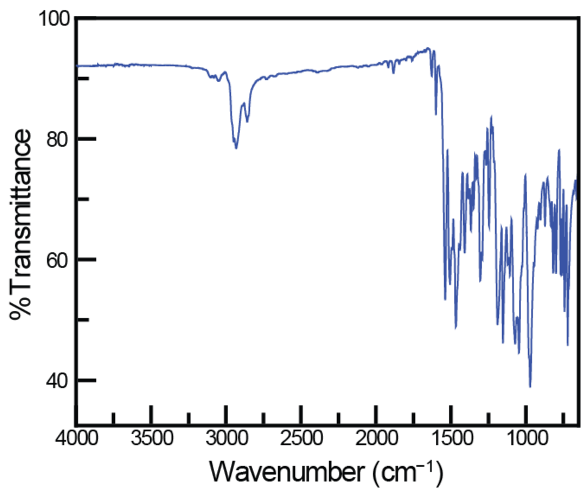

Figure S21. ATR-FT-IR of ***meso*BDP-Carb**

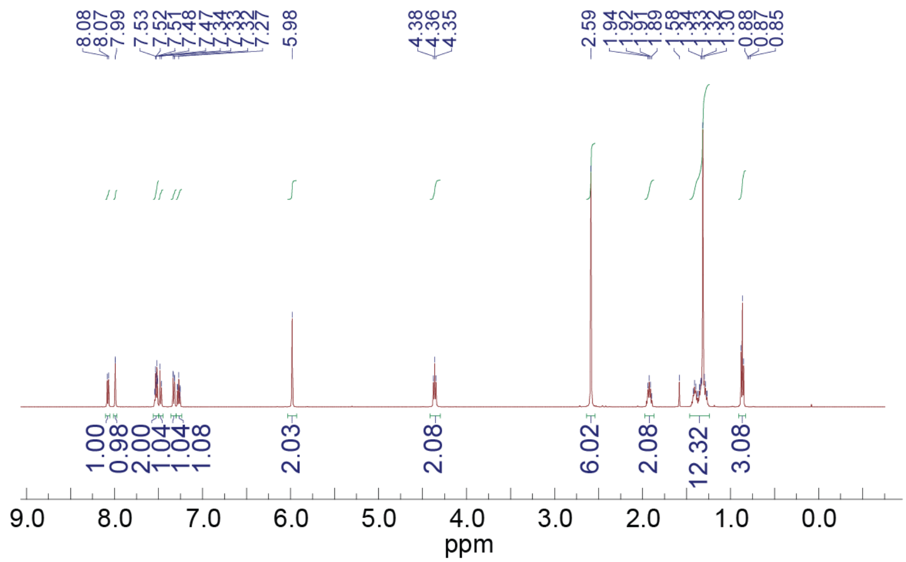

Figure S22. ^{1}H NMR of ***meso*BDP-Carb**

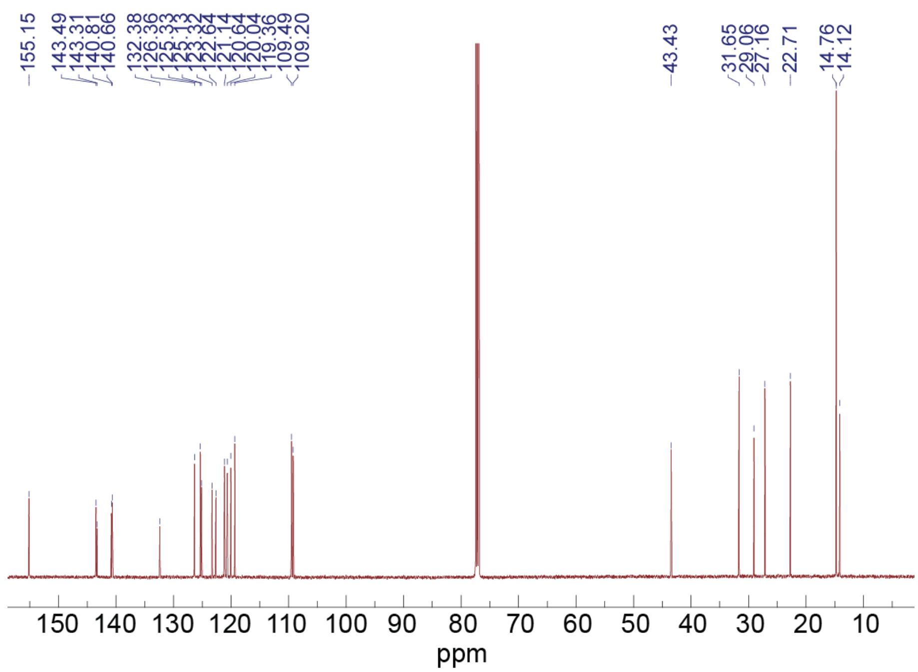

Figure S23. ^{13}C of ***meso*BDP-Carb**

4-Bromophenyl BDP (7)

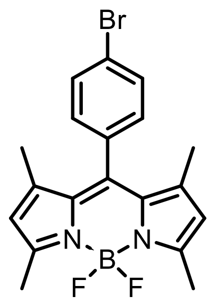

4-Bromobenzaldehyde (0.5 g, 2.6 mmol) was dissolved in dry CH_2Cl_2 (200 ml) and the solution was sparged with Ar. 2,4-dimethylpyrrole (0.5 g, 5.25 mmol) was added *via* a syringe and the contents were sparged for additional 5 min. Trifluoroacetic acid (0.1 mL) was added to the flask and the contents were stirred at room temperature for 1.5 h. The reaction was then quenched with 0.1 N NaOH solution and the organic fraction was washed with water, dried over anhydrous $MgSO_4$ and concentrated *in vacuo*. The residue was dissolved in dry toluene (12 mL) and the flask was purged with Ar. Chloranil (723 mg, 2.9 mmol) was added all at once and the reaction was stirred at room temperature for 5 min. Then, Et_3N (3 mL) and $BF_3.OEt_2$ (3 mL) were added at once and the reaction was stirred for 1.5 h. The reaction mixture was concentrated under reduced pressure and the residue was purified by silica gel chromatography using Combiflash Rf-200 automated flash chromatograph with hexanes-ethyl acetate as the eluents. Evaporation of the solvents yielded the product as an orange-red solid (262 mg, 25%). ^{1}H NMR (400 MHz; $CDCl_3$): δ ppm 7.64 (*d*, J = 8.6 Hz, 2H), 7.18 (*d*, J = 8.6 Hz, 2H), 5.99 (*s*, 2H), 2.55 (*s*, 6H), 1.41 (*s*, 6H).

***meso*BDP-*phen*-Carb (11)**

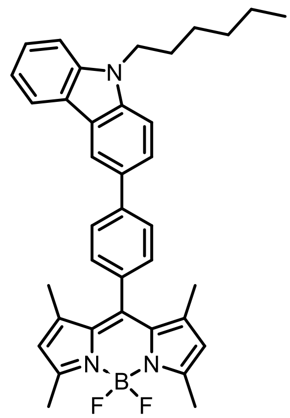

4-bromophenyl BDP (**7**) (88 mg, 0.22 mmol) and *N*-Hexyl-2-(4,4,5,5-tetramethyl-1,3,2-dioxaborolan-2-yl)-carbazole **5** (206 mg, 0.55 mmol) were placed in a 25 mL round bottom flask. To this were added $Pd_2(dba)_3$ (13 mg, 10 mol%), $P(t\text{-}Bu)_3.HBF_4$ (26 mg, 40 mol%) and K_2CO_3 (121 mg, 0.9 mmol). Finally, the solids were suspended in THF (10 mL) and H_2O (2 mL). The contents of the flask were then heated to reflux and stirred for 24 h. The reaction mixture was passed through a short Celite plug and dried over anhydrous $MgSO_4$. After concentration *in vacuo*, the crude product was purified by silica gel chromatography using Combiflash Rf-200 automated flash chromatograph with hexanes-ethyl acetate as the eluents. The final product was further purified by recrystallization from CH_2Cl_2/MeOH to yield an orange-red solid (37 mg, 30%). UV-vis (toluene): λ_{max} = 504 nm, ε = 75,000 $M^{-1}cm^{-1}$ ATR-FT-IR (cm^{-1}): 3051-3045 (w, sp^2 C–H) 2980-2817 (s, sp^3 C–H) ^1H NMR (500 MHz; $CDCl_3$): δ ppm 8.41 (*d*, *J* = 1.6 Hz, 1H), 8.17 (*d*, *J* = 7.6 Hz, 1H), 7.87 (*d*, *J* = 8.4 Hz, 2H), 7.80 (*dd*, *J* = 8 Hz, 2 Hz, 1H), 7.51-7.44 (*m*, 4H), 7.38-7.36 (*m*, 3H), 6.00 (*s*, 2H), 4.35 (*t*, *J* = 7.2 Hz, 2H), 2.58 (*s*, 6H), 1.90 (*quintet*, J = 7.2 Hz, 2H), 1.45-1.28 (*m*, 6H), 1.25 (*s*, 6H), 0.87 (*t*, *J* = 7.2 Hz, 3H). ^{13}C {^1H} NMR (125 MHz $CDCl_3$): δ ppm 155.39, 143.30, 142.79, 142.62, 141.95, 140.94, 140.25, 132.88, 131.61, 130.87, 128.43, 127.89, 127.66, 126.00, 124.92, 123.46, 122.89, 121.22, 120.49, 119.08, 118.86, 109.11, 109.00, 43.29, 31.66, 29.77, 29.03, 27.04, 22.62, 14.73, 14.69, 14.11

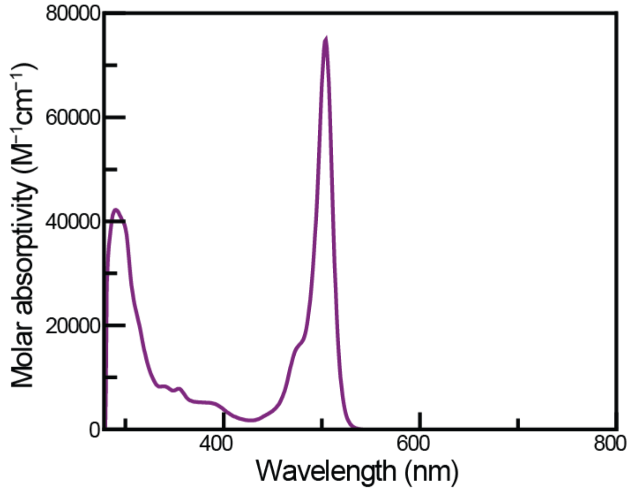

Figure S24. UV-Vis (molar absorptivity) of ***meso*BDP-*phen*-Carb** in toluene

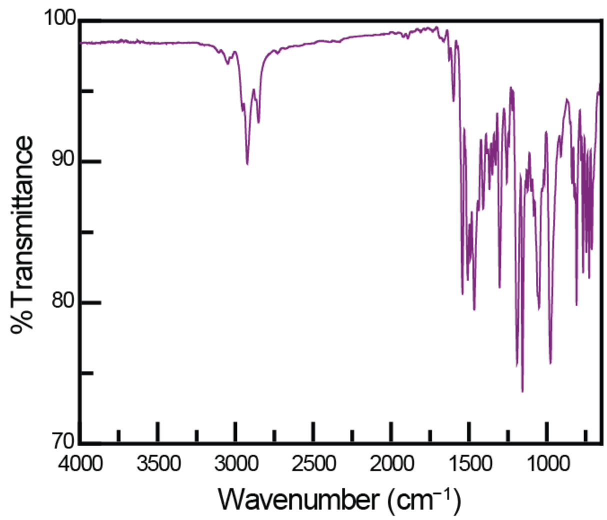

Figure S25. ATR-FT-IR of ***meso*BDP-*phen*-Carb**

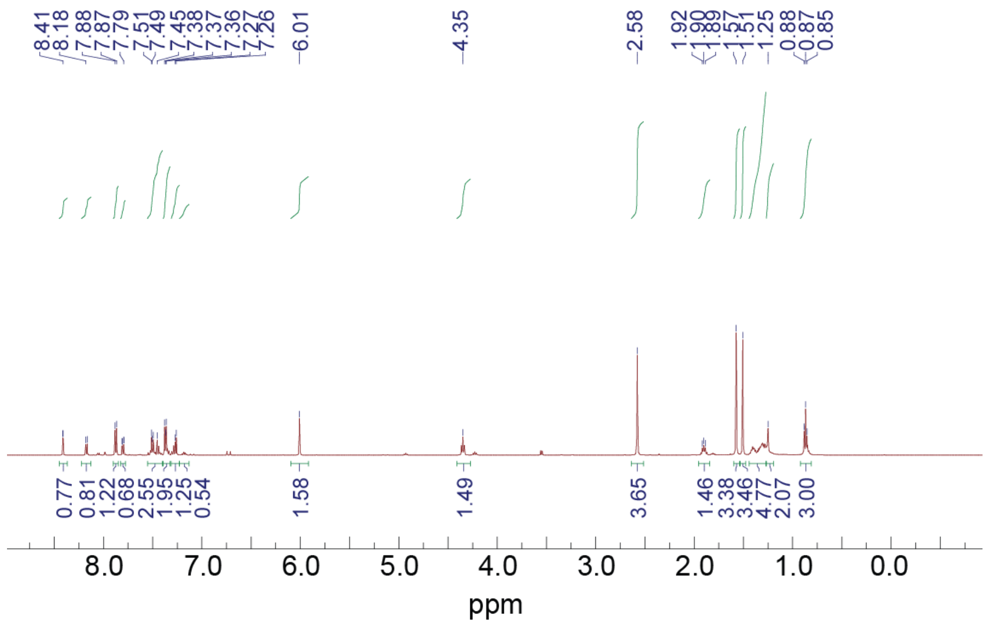

Figure S26. [1]H NMR of ***meso*BDP-*phen*-Carb**

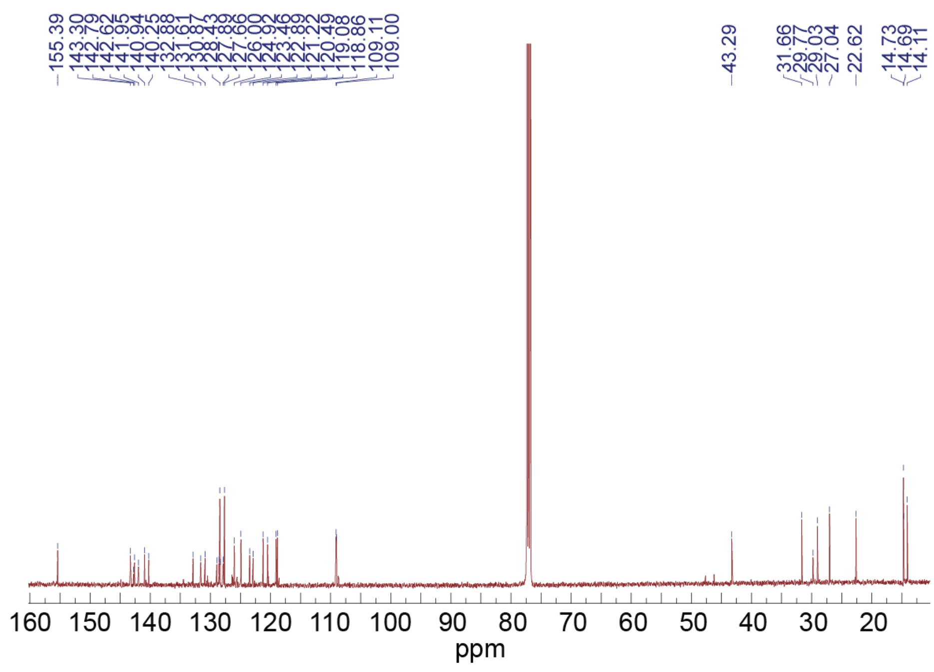

Figure S27. [13]C of ***meso*BDP-*phen*-Carb**

Crystallographic Details

Single crystals of $C_{31}H_{34}BF_2N_3$ **(*meso*BDP-Carb)** were grown from slow evaporation of chloroform. A Brucker D8 Quest diffractometer was used. The crystal was kept at 150.0 K during data collection. Using Olex2[4], the structure was solved with the XT[5] structure solution program using Intrinsic Phasing and refined with the olex2.refine[6] refinement package using Gauss-Newton minimisation.

Table 1 Crystal data and structure refinement for *meso*BDP-Carb.

Identification code	mesoBDPCarb
Empirical formula	$C_{31}H_{34}BF_2N_3$
Formula weight	497.46
Temperature/K	150.0
Crystal system	triclinic
Space group	P-1
a/Å	10.053(4)
b/Å	11.375(4)
c/Å	12.746(6)
α/°	111.34(2)
β/°	105.576(18)
γ/°	90.796(16)
Volume/Å^3	1297.6(10)
Z	2
ρ_{calc}g/cm^3	1.2731
μ/mm^{-1}	0.084
F(000)	528.2
Crystal size/mm^3	0.3 × 0.1 × 0.07
Radiation	Mo Kα (λ = 0.71073)
2Θ range for data collection/°	6.08 to 55.14
Index ranges	$-13 \le h \le 13$, $-14 \le k \le 14$, $-16 \le l \le 16$
Reflections collected	26242
Independent reflections	5976 [R_{int} = 0.0381, R_{sigma} = 0.0348]
Data/restraints/parameters	5976/0/339
Goodness-of-fit on F^2	1.040
Final R indexes [I>=2σ (I)]	R_1 = 0.0446, wR_2 = 0.1034
Final R indexes [all data]	R_1 = 0.0677, wR_2 = 0.1158
Largest diff. peak/hole / e Å^{-3}	0.42/-0.32

Calculated Transitions from Time-Dependent Density Functional Theory

*meso*BDP-Carb

Excited State	energy (eV)	wavelength (nm)	Oscillator strength	from orbital	to obrital	Orbital Contribution
1	2.5346	489.16	0.0002	111	->113	0.6758
				112	->113	-0.18002
2	2.9156	425.24	0.4163	109	->113	0.1134
				110	->113	0.32084
				111	->113	0.13378
				112	->113	0.6076
3	2.9795	416.12	0.1685	110	->113	0.62448
				111	->113	-0.13589
				112	->113	-0.29754
4	3.4784	356.44	0.0621	109	->113	0.69438
				112	->113	-0.12223
5	3.7206	333.24	0.0461	108	->113	0.70409
6	3.875	319.96	0.0431	110	->115	-0.14315
				111	->114	0.63795
				112	->114	-0.25477
7	3.9731	312.06	0.0204	111	->114	0.25579
				112	->114	0.65488
8	3.9839	311.22	0.0004	107	->113	0.69863
9	4.3827	282.89	0.1577	110	->114	0.60545
				111	->115	0.3235
10	4.7706	259.89	0.0076	105	->113	0.6964
11	4.78	259.38	0.1445	106	->113	0.24367
				112	->115	0.63989
				112	->116	0.10651
12	4.8069	257.93	0.7955	106	->113	0.5117
				110	->114	0.12627
				111	->115	-0.39181
				112	->115	-0.19885
				112	->117	-0.10563
13	5.044	245.8	0.3807	106	->113	0.32739
				109	->114	-0.19793
				110	->114	-0.25994
				110	->116	0.12578
				111	->115	0.43645
				111	->117	-0.13719
				112	->115	-0.12241

				112	->117	-0.11988
				112	->118	0.10364
14	5.1013	243.05	0.023	109	->114	0.66855
				111	->115	0.1239
15	5.2095	237.99	0.03	107	->114	0.11814
				110	->115	0.57903
				111	->114	0.10861
				111	->116	-0.31836
16	5.3116	233.42	0	108	->114	0.70443
17	5.3372	232.3	0.1067	107	->114	0.58797
				110	->114	0.14192
				110	->116	0.28055
				111	->116	0.1232
18	5.3983	229.67	0	103	->113	0.42598
				104	->113	0.55687
19	5.5382	223.87	0.0756	107	->114	-0.10468
				111	->117	-0.1221
				112	->115	-0.11179
				112	->116	0.64287
				112	->117	0.1741
20	5.6087	221.06	0.2474	110	->115	0.13232
				110	->116	-0.13111
				111	->116	0.37308
				111	->117	0.38741
				111	->118	0.18262
				112	->116	0.18092
				112	->117	-0.26844
21	5.6813	218.23	0.0002	99	->113	0.12406
				103	->113	0.55441
				104	->113	-0.41463
22	5.7285	216.43	0.2626	105	->114	-0.18594
				107	->114	-0.11382
				110	->115	0.25936
				111	->116	0.44126
				111	->117	-0.32309
				112	->116	-0.10322
				112	->117	0.14608
23	5.821	212.99	0.0476	106	->113	0.14821
				111	->117	0.32315
				112	->117	0.55715
				112	->118	0.13678

24	5.9101	209.78	0.024	107	->114	0.15367
				109	->115	-0.24025
				110	->116	-0.28956
				110	->117	-0.12118
				111	->117	-0.26866
				111	->118	0.44323
				112	->117	0.10207
				112	->118	-0.11514
25	5.9338	208.95	0.0179	109	->115	0.64518
				109	->116	0.10384
				110	->116	-0.15326
				111	->118	0.15232
26	6.0173	206.05	0.0561	100	->113	-0.2905
				101	->113	0.22611
				102	->113	-0.25536
				105	->114	0.16583
				110	->116	0.15366
				110	->117	0.20591
				110	->118	0.11492
				111	->118	0.32471
				112	->118	0.22028
27	6.0401	205.27	0.0777	100	->113	0.27428
				101	->113	-0.35182
				102	->113	0.13913
				105	->114	0.11368
				107	->115	-0.11677
				110	->117	0.18932
				112	->118	0.42078
28	6.0564	204.72	0.0014	106	->114	0.69276
29	6.1059	203.06	0.0064	100	->113	-0.14723
				102	->113	-0.21051
				105	->114	-0.17143
				105	->115	-0.10482
				110	->116	-0.16708
				110	->117	-0.34177
				110	->118	-0.12222
				111	->118	-0.10643
				112	->118	0.41189
30	6.1352	202.09	0.0003	108	->115	0.68453
				108	->116	0.11171
				112	->119	-0.10523

*meso*BDP-*phen*-Carb

Excited State	energy (eV)	wavelength (nm)	Oscillator Strength	from orbital	to obrital	Orbital Contribution
1	2.439	508.34	0.0024	132	->133	0.69865
2	2.8762	431.07	0.55	128	->133	0.14345
				131	->133	0.69529
				131	<-133	-0.10485
3	2.9949	413.98	0.0002	130	->133	0.70065
4	3.3707	367.83	0.081	128	->133	0.68868
				131	->133	-0.14671
5	3.5316	351.07	0.0002	125	->133	0.16357
				129	->133	0.67425
6	3.648	339.87	0.0467	127	->133	0.70407
7	3.7712	328.77	0.0329	130	->135	0.15941
				132	->134	0.66461
				132	->135	-0.13198
8	3.7997	326.3	0.0039	126	->133	0.70593
9	3.9861	311.04	0.5101	130	->134	-0.18963
				132	->134	0.14178
				132	->135	0.65613
10	4.1253	300.54	0.0002	131	->134	0.39175
				131	->135	0.583
11	4.289	289.07	0.0007	125	->133	0.67891
				129	->133	-0.17603
12	4.3242	286.72	0.0022	131	->134	0.58216
				131	->135	-0.38817
13	4.3709	283.66	0.9894	129	->134	-0.11174
				130	->134	0.62549
				130	->135	0.13033
				132	->135	0.18445
				132	->137	-0.11172
14	4.4124	280.99	0.007	126	->135	0.12573
				132	->136	0.67586
15	4.5432	272.9	0.0032	123	->133	-0.1554
				131	->136	0.67705
16	4.591	270.06	0.0995	130	->135	0.63268
				132	->134	-0.15289
				132	->137	0.23411
17	4.8274	256.83	0.1809	123	->133	0.45245
				124	->133	-0.45085
				131	->136	0.16574
				131	->138	-0.17916

18	4.8334	256.52	0.0154	123	->133	0.46272
				124	->133	0.52092
19	4.9495	250.5	0.0012	126	->135	0.10752
				130	->136	0.6719
20	5.049	245.56	0.0829	129	->134	-0.43985
				129	->135	0.10338
				130	->135	-0.14596
				130	->139	0.12616
				132	->137	0.45499
21	5.12	242.16	0.3918	129	->134	0.39131
				129	->135	-0.27137
				130	->134	0.16576
				130	->135	-0.11448
				130	->137	0.12138
				132	->137	0.40007
22	5.1814	239.29	0.047	126	->135	0.12457
				128	->134	0.3561
				128	->135	0.49643
				129	->134	-0.1105
				129	->136	-0.1849
				130	->136	-0.13956
23	5.2688	235.32	0.082	129	->134	0.28779
				129	->135	0.56322
				132	->139	0.14609
				132	->140	-0.11426
24	5.3172	233.17	0.0108	125	->136	-0.1365
				126	->134	0.21286
				126	->135	0.39378
				128	->134	-0.26855
				128	->135	-0.18015
				129	->136	-0.35308
				130	->136	-0.11408
				132	->136	-0.10458
25	5.3597	231.33	0.0051	126	->134	0.17274
				128	->134	0.51659
				128	->135	-0.43294
26	5.3897	230.04	0.0068	129	->135	0.19559
				130	->137	0.48998
				132	->139	-0.3888
27	5.4168	228.89	0	121	->133	0.65154
				122	->133	0.2473

28	5.4531	227.37	0	127	->134	0.4103
				127	->135	0.57042
29	5.4609	227.04	0	131	->137	0.69527
30	5.5917	221.73	0.001	126	->134	0.60843
				126	->135	-0.26404
				128	->134	-0.10904
				128	->136	0.16657

*meso*BDP-*alk*-Carb

Excited State	energy (eV)	wavelength (nm)	Oscillator strength	from orbital	to obrital	Orbital Contribution
1	2.4661	502.76	0.7466	117	->119	0.7044
2	2.6794	462.72	0.4615	118	->119	0.70393
				118	<-119	-0.10184
3	2.9223	424.27	0.0737	116	->119	0.70201
4	3.1737	390.67	0.0289	115	->119	0.69848
5	3.4059	364.03	0.0115	113	->119	0.52345
				114	->119	0.4705
6	3.615	342.97	0.3107	113	->119	-0.46328
				114	->119	0.50436
				117	->120	-0.1163
7	3.8583	321.35	0.0345	114	->119	0.10958
				116	->121	-0.13269
				117	->120	0.67052
8	3.8595	321.24	0	111	->119	0.70252
9	4.0827	303.68	0.0026	118	->120	0.70446
10	4.329	286.41	0.0102	112	->119	-0.16444
				116	->120	0.47051
				117	->121	0.48009
11	4.4286	279.96	0.2283	112	->119	0.61551
				116	->120	0.28648
				117	->121	-0.1002
12	4.5228	274.13	0.0648	118	->121	0.70034
13	4.7508	260.97	0.0693	110	->119	0.6747
				116	->120	0.11099
				116	->121	-0.10562
				117	->121	-0.10462
14	4.83	256.7	0.6045	112	->119	0.26411
				114	->120	-0.19236
				116	->120	-0.33555

				116	->122	0.14921
				117	->121	0.45392
15	5.0496	245.53	0.0689	114	->120	-0.11042
				116	->121	0.59438
				117	->120	0.11611
				117	->122	-0.30844
16	5.1217	242.08	0.1905	114	->120	0.54338
				115	->120	-0.33876
				116	->120	-0.14418
				117	->121	0.10743
17	5.1441	241.02	0.0422	114	->120	0.30109
				115	->120	0.61725
18	5.3165	233.21	0	108	->119	0.70194
19	5.3709	230.84	0.0193	113	->120	0.65021
				114	->120	0.15975
				117	->122	0.17592
20	5.4074	229.28	0.1181	109	->119	0.15387
				113	->120	-0.16915
				116	->121	0.24048
				117	->122	0.51508
				117	->123	0.18975
				118	->123	-0.10164
				118	->124	0.13676
21	5.4815	226.19	0.0064	109	->119	0.52686
				117	->122	-0.14778
				118	->122	-0.29323
				118	->123	-0.14759
				118	->124	0.1582
22	5.4904	225.82	0.0006	114	->125	0.1615
				116	->125	0.1193
				117	->125	0.65816
23	5.4968	225.56	0.0033	109	->119	0.25853
				118	->122	0.63053
				118	->124	0.10128
24	5.5675	222.69	0.2287	112	->120	-0.13937
				114	->121	0.27101
				115	->121	-0.10692
				116	->122	-0.30172
				117	->122	-0.14663
				117	->123	0.42572
				117	->124	0.19524

25	5.5819	222.12	0.0038	115	->121	0.68832
26	5.6228	220.5	0	118	->125	0.70242
27	5.6482	219.51	0.0134	114	->121	0.55594
				116	->122	0.20291
				116	->123	0.10489
				117	->123	-0.16852
				118	->123	-0.1556
				118	->124	0.15635
28	5.8261	212.81	0.0167	113	->121	0.59566
				114	->121	0.1792
				116	->122	-0.13339
				117	->123	-0.15482
				118	->123	0.14469
				118	->124	-0.11315
29	5.8335	212.54	0.0001	111	->120	0.67454
				111	->121	-0.18671
30	5.8447	212.13	0.1116	109	->119	0.10606
				110	->120	0.16366
				112	->120	0.30154
				113	->121	0.2007
				116	->122	0.25379
				117	->122	-0.10803
				117	->123	0.40793
				117	->124	-0.17268
				118	->123	0.12437

*beta*BDP-Carb

Excited State	energy (eV)	wavelength (nm)	Oscillator strength	from orbital	to obrital	Orbital Contribution
1	2.5317	489.73	0.2505	115	->117	0.18375
				116	->117	0.67682
2	2.9657	418.06	0.5046	114	->117	0.16459
				115	->117	0.66323
				116	->117	-0.16198
3	3.088	401.5	0.1444	114	->117	0.68362
				115	->117	-0.14701
4	3.5251	351.72	0.0846	112	->117	-0.18747
				113	->117	0.66629
5	3.7354	331.91	0.0383	111	->117	0.1252
				112	->117	0.67009
				113	->117	0.17238
6	3.7939	326.8	0.032	114	->119	0.13016

				115	->118	0.18863
				116	->118	0.66309
7	4.176	296.89	0.0288	115	->118	0.65738
				116	->118	-0.20177
8	4.2177	293.96	0.0007	111	->117	0.68119
				113	->117	-0.11786
9	4.3777	283.22	0.0325	114	->118	0.55635
				115	->118	-0.10368
				115	->119	-0.17251
				116	->119	-0.36371
10	4.7097	263.25	0.4866	110	->117	0.40852
				114	->118	0.25392
				115	->119	-0.10073
				116	->119	0.46957
11	4.7963	258.5	0.4744	110	->117	0.53254
				114	->118	-0.19405
				115	->121	-0.10282
				116	->119	-0.35115
				116	->121	0.11142
12	4.9033	252.86	0.0058	109	->117	0.69787
13	4.993	248.31	0.1039	113	->118	-0.34796
				114	->118	0.10266
				114	->120	-0.12885
				115	->119	0.56275
14	5.1018	243.02	0.3615	112	->118	0.12248
				113	->118	0.55029
				114	->118	0.18109
				115	->119	0.32604
				116	->120	0.10214
15	5.141	241.17	0.0118	113	->118	-0.12039
				114	->119	0.51422
				115	->120	0.12231
				116	->120	0.40738
16	5.4063	229.33	0.0799	111	->118	0.37558
				112	->118	-0.2504
				114	->118	-0.10711
				114	->119	-0.26093
				114	->120	-0.2139
				116	->120	0.38029
17	5.4618	227	0.2309	111	->118	-0.20875
				112	->118	0.26924

				113	->118	-0.10121
				114	->119	-0.26756
				114	->120	0.24027
				115	->122	0.11357
				116	->120	0.31524
				116	->122	0.24678
18	5.4855	226.02	0.0076	107	->117	0.59615
				108	->117	0.34659
19	5.5408	223.77	0.0496	111	->118	0.25779
				112	->118	0.56683
				113	->118	-0.12601
				114	->120	-0.17023
				116	->122	-0.19226
20	5.6085	221.07	0.0802	110	->117	-0.11451
				111	->118	-0.14522
				116	->120	0.10871
				116	->121	0.61819
				116	->122	-0.1669
21	5.6271	220.33	0.0692	111	->118	0.29509
				113	->119	0.10295
				115	->120	0.35172
				115	->122	0.15274
				116	->120	-0.207
				116	->121	0.16361
				116	->122	0.39899
22	5.74	216	0.1858	109	->118	-0.13662
				114	->119	-0.13251
				115	->120	0.54854
				116	->121	-0.17454
				116	->122	-0.28899
23	5.8099	213.4	0.0232	112	->119	0.13336
				113	->119	0.60258
				114	->120	-0.10506
				114	->122	-0.12717
				115	->121	-0.12493
				116	->121	-0.101
				116	->122	-0.12126
24	5.8491	211.97	0.0132	104	->117	-0.10343
				107	->117	-0.33753
				108	->117	0.58759
25	5.9527	208.28	0.1129	110	->117	0.10848

				115	->121	0.64526
26	5.9695	207.7	0.0189	109	->118	-0.15009
				111	->118	0.27942
				113	->119	0.13708
				114	->120	0.43371
				114	->122	0.14847
				115	->121	0.16035
				115	->122	0.21648
				116	->122	-0.2137
27	6.0316	205.56	0.0022	115	->125	0.16837
				116	->123	0.63792
				116	->125	0.17895
28	6.0865	203.7	0.0151	109	->118	0.21898
				110	->118	-0.27471
				114	->120	-0.15588
				114	->122	-0.20481
				115	->122	0.4973
				116	->122	-0.12436
29	6.1049	203.09	0.0027	103	->117	0.36248
				104	->117	0.27125
				105	->117	0.51427
30	6.1416	201.88	0.0347	109	->118	-0.12176
				110	->118	0.44064
				111	->118	-0.13233
				114	->120	-0.1804
				114	->121	-0.16762
				114	->122	0.22241
				115	->122	0.28541
				116	->124	-0.15741
				116	->125	0.11601

*beta*BDP-*phen*-Carb

Excited State	energy (eV)	wavelength (nm)	Oscillator strength	from orbital	to obrital	Orbital Contribution
1	2.5535	485.54	0.2397	136	->137	0.69765
2	2.9117	425.81	0.6561	135	->137	0.69599
3	3.1884	388.86	0.0521	134	->137	0.69695
4	3.4187	362.67	0.1375	132	->137	0.19093
				133	->137	0.65215
5	3.6721	337.64	0.0513	131	->137	0.24239

				132	->137	0.64053
				133	->137	-0.15501
6	3.7586	329.87	0.0326	134	->139	-0.14159
				135	->138	-0.19701
				136	->138	0.6472
7	3.9846	311.16	0.079	129	->137	-0.12697
				131	->137	0.54778
				132	->137	-0.18045
				133	->137	0.133
				136	->139	0.32295
8	3.9964	310.24	0.0065	130	->137	0.68303
				131	->137	-0.12957
9	4.0099	309.19	0.467	130	->137	-0.14215
				131	->137	-0.28392
				134	->138	0.12579
				136	->139	0.5861
10	4.2122	294.35	0.0997	134	->138	0.24429
				135	->138	0.52238
				135	->139	-0.34834
				136	->138	0.14984
11	4.3359	285.95	0.0027	134	->138	-0.1442
				135	->138	0.38417
				135	->139	0.5262
				136	->138	0.17101
12	4.4375	279.4	0.7057	134	->138	0.56725
				134	->139	-0.1529
				135	->138	-0.11158
				135	->139	0.28569
				136	->139	-0.10605
				136	->141	-0.10514
13	4.4864	276.36	0.0048	130	->139	0.17358
				136	->140	0.66278
14	4.5581	272.01	0.0151	128	->137	-0.14668
				129	->137	0.6582
				131	->137	0.16417
15	4.6576	266.2	0.0568	134	->139	0.62798
				135	->138	-0.11466
				136	->138	0.10786
				136	->141	-0.23001
16	4.789	258.89	0.0912	128	->137	0.56992
				129	->137	0.12273

				135	->140	-0.33948
				135	->142	-0.12027
17	4.824	257.02	0.0372	128	->137	0.30877
				135	->140	0.60951
18	4.9333	251.32	0.0056	133	->138	0.61691
				136	->141	0.25569
19	5.0186	247.05	0.1379	131	->138	0.10644
				133	->139	0.66274
				136	->141	-0.10575
20	5.0509	245.47	0.0026	127	->137	0.68701
				128	->137	-0.13587
21	5.0948	243.35	0.2918	133	->138	-0.24933
				134	->138	0.16935
				134	->139	0.17966
				134	->140	-0.25871
				136	->141	0.50562
22	5.134	241.5	0.0436	130	->139	0.21055
				133	->140	0.13274
				134	->140	0.58441
				136	->140	-0.12411
				136	->141	0.17652
23	5.3245	232.86	0.0351	130	->138	-0.25001
				130	->139	0.32985
				133	->140	0.44969
				134	->140	-0.26755
				136	->140	-0.14035
24	5.3577	231.42	0.0204	131	->138	-0.26315
				131	->139	-0.10378
				132	->138	0.2236
				133	->138	0.10881
				133	->139	0.11325
				134	->141	0.37859
				135	->141	0.14804
				135	->143	-0.10823
				136	->143	0.28533
25	5.4316	228.26	0.0007	130	->138	0.11187
				131	->138	-0.30892
				131	->139	0.13437
				132	->138	0.35901
				132	->139	-0.13662
				135	->141	-0.32698

				135	->143	0.10939
				136	->141	-0.13334
				136	->143	-0.19971
				136	->144	-0.10571
26	5.4637	226.92	0.0025	130	->138	0.61133
				130	->139	0.18567
				131	->139	0.11921
				132	->139	-0.10526
				133	->140	0.1661
				135	->141	0.12243
27	5.4813	226.2	0.0884	130	->138	-0.10603
				131	->139	0.18914
				132	->138	0.1626
				132	->139	-0.1938
				134	->141	-0.11764
				135	->141	0.53184
				136	->143	-0.21861
28	5.4924	225.74	0.0017	124	->137	-0.18952
				125	->137	0.6503
				126	->137	0.15981
29	5.5251	224.4	0.002	130	->138	0.13321
				131	->139	-0.36579
				132	->138	0.14721
				132	->139	0.38885
				134	->141	-0.27
				134	->143	0.12678
				135	->141	0.12793
				136	->143	-0.11017
30	5.6025	221.3	0.0096	131	->138	0.42778
				131	->139	-0.16791
				132	->138	0.4602
				132	->139	-0.19578
				136	->143	0.1278

*beta*BDP-*alk*-Carb

Excited State	Energy (eV)	Wavelength	Oscillator strength	from orbital	to orbital	contribution
1	2.2895	541.54	0.4344	122	->123	0.70053
2	2.9891	414.79	0.4828	120	->123	-0.12031
				121	->123	0.68954
3	3.1548	393.01	0.2249	120	->123	0.69066
				121	->123	0.11506
4	3.4686	357.45	0.1253	118	->123	0.18309
				119	->123	0.66081
5	3.6172	342.76	0.0307	120	->125	-0.11967
				121	->124	0.10697
				122	->124	0.6644
6	3.6655	338.25	0.0631	118	->123	0.66838
				119	->123	-0.18751
7	3.9168	316.54	0.0676	120	->124	0.11254
				122	->125	0.67508
8	4.23	293.11	0.0231	116	->123	-0.37412
				117	->123	0.46503
				120	->124	-0.13371
				121	->124	0.29531
9	4.2345	292.8	0.2544	116	->123	0.22259
				117	->123	-0.25866
				120	->124	-0.24749
				121	->124	0.51035
				121	->125	-0.10242
10	4.3083	287.78	0.0175	116	->123	0.53943
				117	->123	0.43087
11	4.4391	279.3	0.124	120	->124	0.45876
				120	->125	-0.14356
				121	->124	0.30016
				121	->125	0.37593
				122	->124	-0.11617
12	4.5859	270.36	0.3766	119	->124	-0.12139
				120	->124	-0.34484
				120	->125	0.12845
				121	->125	0.54367
				122	->126	0.10539
13	4.7105	263.21	0.1225	115	->123	0.64799
				120	->125	-0.13513
				121	->127	-0.10229
				122	->127	0.10884

14	4.7404	261.55	0.0108	115	->123	0.16009
				120	->125	0.55869
				121	->124	0.12791
				122	->126	-0.33424
15	4.9215	251.92	0.0483	114	->123	-0.18691
				119	->124	0.51589
				119	->125	0.13347
				120	->125	0.18692
				121	->124	0.10757
				122	->126	0.32131
16	4.987	248.62	0.0138	114	->123	0.65926
				119	->124	0.21223
17	5.0717	244.46	0.3896	114	->123	0.12441
				119	->124	-0.34568
				120	->124	0.17747
				120	->125	0.24883
				121	->125	-0.10732
				122	->126	0.46674
				122	->128	0.1198
18	5.1266	241.84	0.007	119	->124	-0.1384
				119	->125	0.62494
				122	->128	0.10739
19	5.2518	236.08	0.0062	119	->129	0.12094
				122	->127	-0.13311
				122	->129	0.58019
				122	->130	-0.19178
				122	->131	-0.20661
20	5.3627	231.2	0.0225	113	->123	-0.28945
				119	->125	-0.10729
				122	->127	0.5799
				122	->129	0.11885
21	5.3828	230.33	0.0806	113	->123	0.14466
				119	->125	-0.14679
				120	->124	-0.10514
				120	->126	-0.24948
				121	->126	0.1496
				121	->128	0.11671
				122	->128	0.53742
22	5.4669	226.79	0.0026	112	->123	0.20207
				115	->125	0.12075
				116	->124	-0.26909

				116	->125	0.53863
				117	->124	0.14143
				117	->125	-0.16936
23	5.519	224.65	0.0821	112	->123	0.51274
				113	->123	-0.34033
				117	->124	-0.12063
				118	->124	0.10931
				122	->127	-0.18104
				122	->128	0.14998
24	5.5423	223.71	0.0765	112	->123	0.38601
				113	->123	0.24019
				116	->125	-0.19387
				117	->124	0.17295
				118	->124	-0.32854
				120	->126	-0.12587
				122	->127	0.10703
				122	->128	-0.19915
25	5.5507	223.37	0.036	112	->123	0.19471
				113	->123	0.4099
				117	->124	-0.18518
				118	->124	0.39578
				120	->126	0.13644
				122	->127	0.19754
26	5.6216	220.55	0.0154	117	->124	0.33354
				118	->124	0.43012
				118	->125	-0.1281
				120	->126	-0.27183
				122	->128	-0.19127
27	5.6639	218.9	0.0247	117	->124	-0.18772
				117	->125	-0.14057
				118	->125	0.23906
				121	->126	0.56818
				122	->128	-0.10419
28	5.717	216.87	0.018	118	->124	0.16382
				118	->125	0.62039
				120	->126	-0.10549
				121	->126	-0.23735
29	5.7769	214.62	0.002	116	->124	0.42208
				116	->125	0.17884
				117	->124	-0.27478
				117	->125	-0.21349

				118	->125	-0.11684
				120	->126	-0.27939
				120	->128	-0.13318
				121	->126	-0.13723
30	5.8338	212.53	0.0017	115	->124	0.16387
				116	->124	0.44141
				116	->125	0.19609
				117	->124	0.25919
				120	->126	0.26887
				120	->128	0.16712
				121	->126	0.10616
				121	->128	-0.10784

1. Nepomnyashchii, A.; Bröring, M.; Ahrens, J.; Bard, A. J.: Synthesis, Photophysical, Electrochemical, and Electrogenerated Chemiluminescence Studies. Multiple Sequential Electron Transfers in BODIPY Monomers, Dimers, Trimers, and Polymer. *J. Am. Chem. Soc.* **2011**, *133*, 8633–8645.
2. Rihn, S.; Erdem, M.; De Nicola, A.; Retailleau, P.; Ziessel, R.: Phenyliodine(III) Bis(trifluoroacetate) (PIFA)-Promoted Synthesis of Bodipy Dimers Displaying Unusual Redox Properties. *Org. Lett.* **2011**, *13*, 1916–1919.
3. Grisorio, R.; Piliego, C.; Fini, P.; Cosma, P.; Mastrorilli, P.; Gigli, G.; Suranna, G. P.; Nobile, C. F.: Influencing the Spectral Stability and the Electroluminescence Behavior of New Blue-Emitting Bifluorene-Based Materials by the 7,7′-Functionalization of the Core. *J. Phys. Chem. C* **2008**, *112*, 7005-7014.
4. Dolomanov, O.V., Bourhis, L.J., Gildea, R.J, Howard, J.A.K. & Puschmann, H. (2009), J. Appl. Cryst. 42, 339-341.
5. Sheldrick, G.M. (2015). Acta Cryst. A71, 3-8.
6. Bourhis, L.J., Dolomanov, O.V., Gildea, R.J., Howard, J.A.K., Puschmann, H. (2015). Acta Cryst. A71, 59-75.